

Dynamic concentration of motors in microtubule arrays

François Nédélec*, Thomas Surrey* and Anthony Maggs†

*EMBL, Cell Biology, Meyerhofstrasse 1, 69115 Heidelberg, Germany

†ESPCI, PCT, 10 Rue Vauquelin, 75005 Paris, France

We present experimental and theoretical studies of the dynamics of molecular motors in microtubule arrays and asters. By solving a convection-diffusion equation we find that the density profile of motors in a two-dimensional aster is characterized by continuously varying exponents. Simulations are used to verify the assumptions of the continuum model. We observe the concentration profiles of kinesin moving inwards in quasi two-dimensional artificial asters by fluorescent microscopy.

The cytoskeleton is a network of polymers essential for the dynamic organization of many eukaryotic cells. Its function depends not only on protein fibers, but also on many accessory components [1]. Among these are motor proteins that bind to and walk along the surface of cytoskeletal polymers, consuming ATP as a source of energy. A natural consequence of this directed movement in organized fiber arrays is a non-uniform spatial distribution of the motors. We observe for example that kinesin molecules concentrate in arrays of microtubules. In this paper we model and calculate the stationary density profiles of motors in a fixed distributions of fibers.

In vivo microtubules are often observed in radial arrays, or asters, where all microtubule “minus” ends are at the center, and the “plus” ends are radiating outward. Aster of opposite polarity, in which kinesin moves inward can also be formed in-vitro [16]. Here we consider isotropic asters, in one, two and three dimensions Fig. (1). The “degenerate” aster in one dimension corresponds to a tube in which microtubules are all oriented in the same direction. This is the case for example in the axons of nerve cells. As distinct motors move toward the “plus” or the “minus” end, we consider both cases of inward/outward directed motion.

Consider N immobile straight microtubules, Fig. (1). The filaments are radial and arranged isotropically in the available volume of dimensions $d=1,2$ or 3 . Molecular motors are present which can exist in two different states, either attached to a filament, or detached. Unattached motors diffuse freely, with a diffusion constant D . Attached motors move on their filament (radially in the aster geometry) at a speed v , which can be either positive or negative. Positive values of v corresponds to outward movement. Transitions between the two motor states are stochastic. The motor can spontaneously detach from the microtubule at an unbinding rate p^{off} (s^{-1}). Far from saturation, the number of binding events per second is proportional to the local concentration of free motors, and to the number of available binding sites on the microtubules. If the concentration of free motors is expressed in molecules per cubic micrometers, and the available “quantity” of microtubules in micrometers, the constant of proportionality p^{on} has the dimension of a diffusion constant [2,3].

Let $b(r)$ and $f(r)$ be the concentrations of bound and free motors, respectively, at distance r from the center.

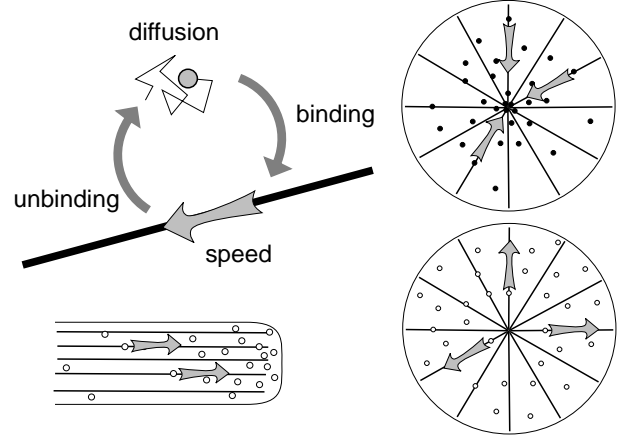


FIG. 1. In the presence of a microtubule array motors can move by free diffusion in solution or by directed motion on microtubules. Movement of motors in an aster can lead to accumulation, if the motor moves inward (top right), or depletion, if the motor moves outward (bottom right). Accumulation also occurs in oriented parallel microtubule arrays (bottom left).

Bound motors move radially at speed v , and create a convective flux $J_b = vb$. Unbound motors diffuse freely, creating a radial flux $J_f = -Ddf/dr$. If S is the surface area at distance r , there are $p^{\text{off}}Sbdr$ release events in the volume between the radii $[r, r + dr]$, and $p^{\text{on}}Nfdr$ attachments per second. We therefore obtain the coupled kinetic equations:

$$\begin{aligned}\frac{\partial b}{\partial t} &= -p^{\text{off}}b + \frac{p^{\text{on}}N}{S}f - \frac{1}{S}\frac{\partial}{\partial r}(J_bS) \\ \frac{\partial f}{\partial t} &= +p^{\text{off}}b - \frac{p^{\text{on}}N}{S}f - \frac{1}{S}\frac{\partial}{\partial r}(J_fS)\end{aligned}\quad (1)$$

To find the steady state, we use the fact that the net flux $J_b + J_f$ is zero, implying $b = Dv^{-1}(df/dr)$. Substituting this result into equation (1), and denoting $f' = df/dr$ and $f'' = d^2f/dr^2$, we find in d dimensions

$$\begin{aligned}0 &= f'' + \left(\frac{1}{\alpha} + \frac{d-1}{r}\right)f' - \frac{1}{r^{d-1}\beta_d}f \\ b &= \gamma f'\end{aligned}\quad (2)$$

The physical parameters in the problem have been reduced to

$$\begin{aligned} \alpha &= v/p^{\text{off}} \\ \beta_1 &= S_1 D/p^{\text{on}} N, \quad \beta_2 = 2\pi h D/N p^{\text{on}}, \quad \beta_3 = 4\pi D/p^{\text{on}} N \\ \gamma &= D/v. \end{aligned} \quad (3)$$

where S_1 is the area of the tube in one dimension and h is the sample thickness in a quasi two-dimensional geometry. α is the average distance that a motor moves on a microtubule, before detaching. β_d characterizes the geometry of the aster, and γ determines the relative concentration of bound to free motors. Note that for inward movement, α and γ have negative values, while for outward movement all parameters are positive.

For the motor protein kinesin, experimental data provide values for the parameters in the model. The walking speed of kinesin without load is $v = 0.8 \mu\text{ms}^{-1}$ [5,6]. The unbinding rate p^{off} is obtained from the average distance that kinesin moves before detaching. Measured average run length, $\alpha = v/p^{\text{off}}$, are for kinesin in the range $0.4 - 1.5 \mu\text{m}$ [7-9]; we use $p^{\text{off}} = 1 \text{ s}^{-1}$. Direct chemical measurements of p^{off} [3] agree with this value. The binding rate p^{on} of the kinesin construct used in our experiment has not been directly measured. To estimate it, we assume that interaction between microtubules and motors is diffusion limited [10]): Measurements with kinesin's soluble dimeric motor domain [3] provide a value of $p^{\text{on}}_{\text{kin}} = 7.3 \mu\text{m}^2\text{s}^{-1}$, and its diffusion constant is $50 \mu\text{m}^2\text{s}^{-1}$ [11,12]. For single kinesin adsorbed on beads [9], the equilibrium constant for the binding convection (equal to $p^{\text{on}}/p^{\text{off}}$), provides $p^{\text{on}}_{\text{bead}} = 0.25 \mu\text{m}^2\text{s}^{-1}$, and a diffusion constant of $2 \mu\text{m}^2\text{s}^{-1}$ [13]. The ratios p^{on}/D are 0.14 and 0.12 respectively, and we use the averaged value $p^{\text{on}}/D = 0.13$. Finally, based on its molecular weight, we estimated a diffusion constant of $D = 20 \mu\text{m}^2\text{s}^{-1}$ for the construct used in our experiment [14], which yields $p^{\text{on}} = 2.6 \mu\text{m}^2\text{s}^{-1}$.

In a tubular, quasi one dimensional geometry, all microtubules are oriented in the same direction, (Fig 1), lower left. We find that the steady state profile for the motor concentration is exponential $f(r) \sim e^{r/a}$ where the distance a is a root of the equation $a^2 + a/\alpha - 1/\beta_1 = 0$. The ratio of bound to free motors is constant along the tube, and equal to γ/a . To relate this result to the situation of motors in a cell, we now consider a tube filled with oriented microtubules connected on one side to a large body. Motors have a concentration which varies exponentially with the distance from the cell body. The concentration at the end of the tube is $e^{L/a}$ times smaller (or greater depending on the motor sense) than in the cell body, where L is the length of the tube. We estimated a for a cellular extension of a diameter of $2 \mu\text{m}$, and for parameters of the motor kinesin: If the extension contains 20 microtubules, then $a = 2 \mu\text{m}$; for the same tube containing a single microtubule, $a = 30 \mu\text{m}$. Therefore an unregulated kinesin (which can always bind and move) would be concentrated even in short extensions of a cell containing outward polarized microtubules. This is indeed observed *in vivo* for kinesin heavy chain if it is over-expressed in the absence of the regulatory light

chain [4].

We now consider a two dimensional aster. Because of the radial geometry the situations of motors moving inward, and of motors moving outward are not symmetric. This is easily seen by considering a non-motile binding protein ($v = 0$). At equilibrium, the unbound molecules are evenly distributed throughout the volume, $f(r) = \text{const}$, while the concentration of bound molecules is proportional to the local concentration of microtubule so that $b(r) \sim 1/r$. Thus, in the geometry of the aster, binding of motors induces their accumulation in the center, where microtubules are more concentrated. This helps the concentration of motors moving inwards, and has to be overcome by motors moving outwards before depletion.

The solutions can be expressed in terms of Whittaker functions, however asymptotic analysis shows that the solution in the quasi-two dimensional case is well approximated by the power laws beyond the radius α^3/β_2^2 : $f(r) \sim r^{\alpha/\beta_2}$, and $b(r) \sim \gamma f(r)/r$. Thus the concentration profile of motors is characterized by an exponent which is a continuous function of the physical parameters. From the above expressions we find $\alpha = \pm 0.8 \mu\text{m}$, $1 \mu\text{m} < \beta_2 < 10 \mu\text{m}$, and $\gamma = \pm 60 \mu\text{m}$.

For typical values of the parameters in two dimensions we find a 10 fold increase in the concentration of motors, within a few micrometers from the center [15]. The theory allows us to calculate a critical number of microtubules above which the concentration of free motors decreases faster than $1/r$. Then most of the motors are trapped in the center of the aster, and very few motors are left elsewhere in the sample. For kinesin, and a sample thickness of $9 \mu\text{m}$ this dynamical segregation occurs above ~ 600 microtubules, a very reasonable value experimentally. The depletion from the aster center of a kinesin motor moving outwards is comparatively weaker. As noted above motors are concentrated in the center, merely as a consequence of the binding of motors to microtubules. Total depletion is achieved only for large asters (of 1000 microtubules), for which outward transport overcomes the pure binding effect. Depending on the number of microtubules in the aster, the same outward-moving motor can be either concentrated or depleted.

In three dimensions, motors are depleted or concentrated only within a finite distance $\alpha/\sqrt{\beta_3}$, from the center of the aster. The concentrating power of an aster is too weak in three dimensions to have a strong effect over a whole sample volume.

To derive the convection-diffusion equations, we averaged over the directions transverse to the microtubules (both angularly, and over the thickness of the sample). This approximation can break down at the center of the aster, where the geometry is really three-dimensional; or at large radial distances where the microtubules are too far apart for angular averaging. We performed simulations to check that no substantial errors are introduced in the theoretical description. In our simulations the aster is formed by microtubules of length $L = 50 \mu\text{m}$, with their

“plus” end in the center of a cylindrical box of radius L , and of thickness $9 \mu\text{m}$. Each motor is characterized by its state (bound or free), and a vector (position). To compute the binding of motors, a rate p^+ and an interaction range ϵ were introduced, so that at each step, a free motor has a probability $p^+ dt$ to bind to any filament located at a distance (by projection) closer than ϵ , this effectively corresponds to $p^{\text{on}} = p^+ \pi \epsilon^2$. At each time step $dt = 4 \cdot 10^{-5} \text{s}$, bound motors may detach with a probability $p^{\text{off}} dt$, and otherwise move radially by a distance $v dt$; free motors make random steps, with $\langle dx^2 \rangle = 3D dt$. The motor parameters were taken to mimic kinesin (see above), with the additional value $\epsilon = 50 \text{ nm}$ [9], and $p^+ = 312 \text{ s}^{-1}$ (which yield the correct value for p^{on}). Other choices of ϵ and p^+ conserving p^{on} gave similar curves.

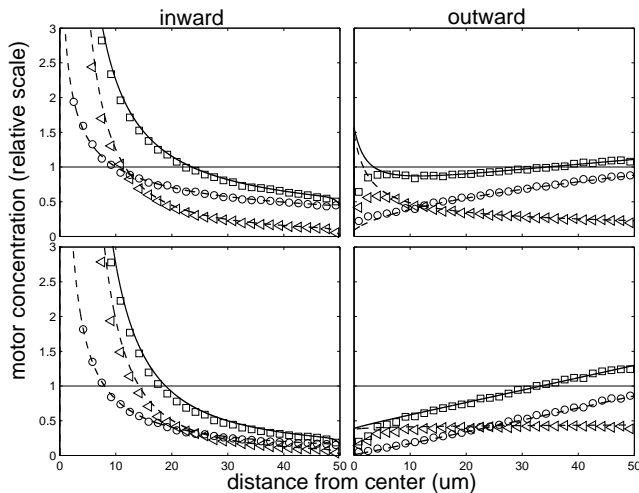


FIG. 2. Simulated bound (triangles), free (circles) and total=bound+free (squares) motor concentrations and theory (lines), for kinesin moving inward (left) or outward (right) in asters having either 300 (top) or 600 (bottom) microtubules. The relative concentrations of bound to free motors varies with the distance from the center of the aster. As expected some deviations are seen near the center of the aster.

The simulation was a direct implementation of the model, and the agreement with theory, Fig. (2) confirms that our analytical approximations are faithful to the model.

Using fluorescent microscopy we measured the kinesin distribution in asters with both possible polarities. These asters with either the plus or the minus ends of the microtubules in the center are formed by multimeric complexes of motors [14,16], and take about 30 minutes to form. All data presented here are extracted from two identically prepared samples, in which many asters of various size formed. We measured 115 regular asters with an automatic epi-fluorescence microscopic setup (Zeiss axio-plan 2 with Olympus 100X oil-immersion objective). We detected the motors (labeled with the fluorophore fluorescein) and the microtubules (labeled with rhodamine)

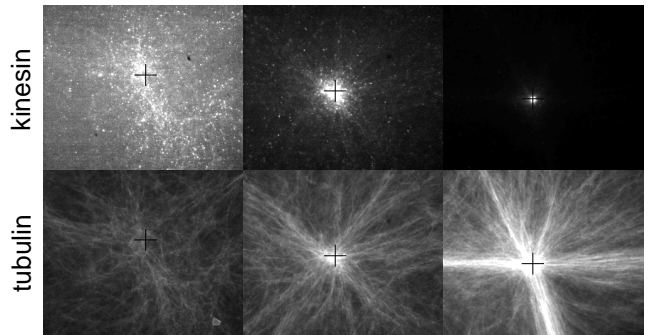


FIG. 3. Motor and microtubule distribution in experimental asters with different number of microtubules: Fluorescence images ($90 \times 70 \mu\text{m}$) obtained for the motors (top), for the microtubules (middle). The cross mark the computed measured center. The intensities of the images are here scaled by different factors.

independently. Digital pictures were taken with a 12-bit CCD camera (Hamamatsu C4742-95, 1280×1024 pixels). The camera is linear, and unsaturated pixel values reflect the relative quantity of protein in the imaged region. A conversion factor of 70 nm per pixel and a thickness of $9 \mu\text{m}$ were experimentally determined.

The center of the aster and the profiles of fluorescence intensity are calculated automatically. Because of the noise in the data we removed a central portion of radius $1.5 \mu\text{m}$ from the center. A common background pixel value was subtracted from the motor profiles, which are then normalized. To measure the number of microtubules in the aster, we fit the profile of microtubule fluorescence to the function $(M/r + B)$, where r is the distance from the center. B is a background, and M is proportional to the number of microtubules. Calibration was done by manually counting the microtubules in five asters. The $1/r$ profile corresponds to an homogeneous aster of long microtubules. Experimentally the asters are not perfect (some, like Fig 3, left are not well focused). When the fit of the microtubule-profile to $1/r$ is poor, we have no reason to expect the theory to apply. These asters are plotted with a different symbol in Fig. (4).

We measured the distribution of kinesin in concentrating asters containing different numbers of microtubules. Three typical examples are given in Fig. (3). Motor profiles of individual asters are rather well fitted by a power law. They are almost linear on a log-log plot, and steeper for bigger asters Fig. (4, inset). Plotting the exponent of the motor profiles as a function of the number of microtubules extracted from the microtubule profiles allows us to compare directly experiments and theory (see Fig. 4). The data points, each representing one aster, are scattered around the theoretical curve, probably reflecting intrinsic variations and heterogeneity of the asters. However, the major trend in the exponent, characterizing the motor profile, is correctly predicted by the theory, so that denser asters are characterized by a

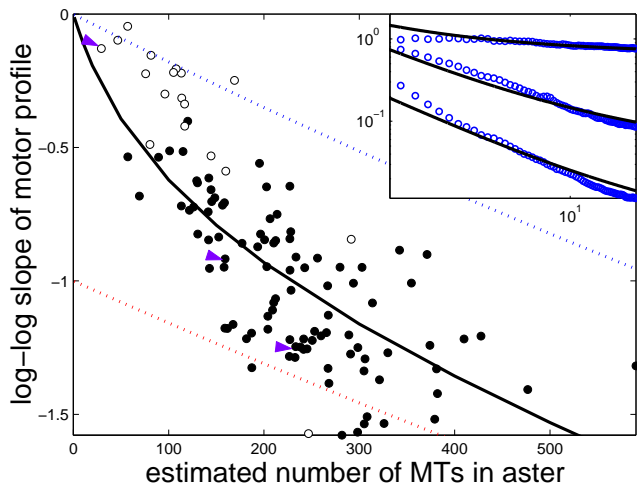


FIG. 4. The effective exponent of the kinesin concentration profile becomes more negative with the increasing numbers of microtubules in the aster (continuous line: theory). Filled symbols correspond to regular asters for which the radial microtubule density falls off as $1/r$. Open symbols correspond to irregular asters where the density is inconsistent with a law in $1/r$. Arrow heads point to asters shown in previous figures. Inset (log-log): Experimental (circles) motor concentration profiles, as extracted from the pictures shown in Fig. 3, and theoretical curves computed for the measured number of microtubules (27, 148, 231) in the aster.

larger localization exponent for the motors.

We also imaged kinesin moving outwards in asters of normal polarity (formed as in [16]), but the signal was too dim to extract a reliable profile. As the predicted kinesin profile in minus-asters with less than 500 microtubules (the maximum achievable number in our experiment) is rather flat, this does not rule out the theory.

Accumulation or expulsion of molecular motors in asters may have important functional implications in biology. For instance within a spindle made of two interacting asters of microtubules, minus-ended motors could concentrate at the poles while plus-ended motors would be excluded from the same regions. This could contribute to the mechanism of spindle assembly, and/or to its mechanical stability. Interestingly we find that kinesin accumulates in asters of 300-1000 microtubules, which is comparable to the number of microtubules present in spindle asters of most animal cells.

We did not consider the regulation of motor activity: In our study motors can always bind and move on filaments. Cells use a variety of processes to counterbalance the impact of motor transport on their localization. For example, the folding of kinesin into a non-motile conformation, in the absence of a cargo [11,17,18] dampens the transport-induced localization. The recombinant kinesin fraction used in our experiment lacks this capacity. Even with this partial inhibition, the movement of loaded ki-

nesin brings them to places from which they have to be recycled. Additional regulation mechanisms include local synthesis and degradation of the motors, involvement of motors of different directionality transporting each other, etc. However, we can also imagine situations in which the unregulated localization of a motors resulting from their movement can be a benefit to the cell.

In summary, motor movements on microtubules can effectively cause their “compartmentalization”. The theory provides a full understanding of the influence of all motor kinetic parameters, and of the geometric properties of the microtubule array. This is a first step towards a more quantitative understanding of the complex dynamics of motor populations.

We thank A. Ajdari, S. Blandin, A. Desai, E. Karsenti and S. Leibler. for discussions and encouragement.

-
- [1] Kreis, T & Vale, R, eds. *Guidebook to the Cytoskeletal and Motor Proteins*. (Oxford University Press, 1993).
 - [2] Foster, K. A, Correia, J. J, & Gilbert, S. P. (1998) *J. Biol. Chem.* **273**, 35307–35318.
 - [3] Hackney, D. *Nature*, **377**, 448–450, (1995).
 - [4] Verhey, K, Lizotte, D, Abramson, T, Barenboim, L, & Schnapp, B. *J. Cell Biol.* **143**, 1053–1066 (1998).
 - [5] Howard, J, Hudspeth, A. J, & Vale, R. D. *Nature*, **342**, 154–158, (1989).
 - [6] Svoboda, K & Block, S. *Cell*, **77**, 773–784, (1994).
 - [7] Block, S. M, Goldstein, L. S, & Schnapp, B. *J. Nature*, **348**, 348–352, (1990).
 - [8] Vale, R. D, Funatsu, T, Pierce, D. W, Romberg, L, Harada, Y, & Yanagida, T. *Nature*, **380**, 451–453, (1996).
 - [9] Coy, D, Wagenbach, M, & Howard, J. *J. Biol. Chem.* **274**, 3667–3671, (1999).
 - [10] Hackney, D. *Biophys J* **68**, 267s–270s, (1995).
 - [11] Hackney, D, Levitt, J, & Suhan, J. *J. Biol. Chem.* **267**, 8696–8701 (1992).
 - [12] Huang, T.-G, Suhan, J, & Hackney, D. *J. Biol. Chem.* **269**(23), 16502–16507, (1994).
 - [13] Hancock, W. O & Howard, J. (1999) *Proc. Natl. Acad. Sci. USA*, **96**, 13147–13152, (1999).
 - [14] Nedelec, F, Surrey, T, Maggs, A, & Leibler, S. *Nature*, **389**, 305–308 (1997).
 - [15] Experimentally, we always observe formation of aggregates (containing kinesin) at the center of the aster, reflecting the finite solubility of the protein.
 - [16] Nedelec, F & Surrey, T. (in-press) *Methods Mol. Biol.*
 - [17] Coy, D. L, Hancock, W. O, Wagenbach, M, & Howard, J. *Nat. Cell. Biolog.* **1**, 288–292, (1999).
 - [18] Stock, M, Guerrero, J, Cobb, B, Eggers, C, Huang, T.-G, Li, X, & Hackney, D. *J. Biol. Chem.* **274**, 14617–14623, (1999).